Available online at www.sciencedirect.com

ScienceDirect

Energy Procedia 155 (2018) 412–430

Energy Procedia

www.elsevier.com/locate/procedia

12th International Renewable Energy Storage Conference, IRES 2018

Dynamic Simulation and Comparison of Different Configurations for a Coupled Energy System with 100 % Renewables

Carsten Bode*, Gerhard Schmitz

Institute of Engineering Thermodynamics, Hamburg University of Technology, Denickestr. 17, 21073 Hamburg, Germany

Abstract

For the successful transition to a renewable energy source powered society, coupling of different energy sectors is inevitable. The extreme case of a future German energy system consisting of power, heat and gas consumers supplied with 100 % renewables is analyzed here. To find the most cost-effective system configuration, different combinations of storage and conversion technologies are compared by performing dynamic simulations and evaluating the average costs over the period of one year.

Renewable power production is modeled by using actual power-generation curves and extrapolating the installed power for each technology according to the German energy system framework. Final energy curves for power, heat and gas demand are created as a result of the study. The gas demand only arises from industries using hydrocarbons as a product in processes and for high temperature process heat.

The components of the energy system, e.g. storage and conversion technologies are modeled using the equation-based open-source TransiEnt Library based on Modelica®.

To obtain the boundaries of the solution scope, the comparison is started by analyzing homogeneous scenarios, e.g. All-Electric or All-Gas with Power-to-Gas with reconversion to power and heat. To find the optimal configuration within this scope, different combinations of power (adiabatic compressed air energy storage (A-CAES), lithium-ion battery, pumped hydro storage), heat storage (hot water storage) and gas storage (underground storage) technologies as well as conversion technologies, i.e. Power-to-Gas (electrolyzer with methanation), Power-to-Heat (electric heat pump, electric boiler), Gas-to-Heat (gas boiler, gas heat pump), and Gas-to-Power (gas turbine, combined cycle gas turbine) are simulated.

The results show that a homogeneous energy system configuration where all services are supplied by either power or gas are technically possible but not economic. Due to the limited technical potential of renewables, ecological feasibility of All-Gas systems is limited. A combination of Power-to-Gas with combined cycle gas turbines, electric heat pumps, a lithium-ion battery and pumped hydro storage is the option with the lowest cost. Using an A-CAES instead of the battery or adding an A-CAES to the battery does not lower the cost.

Keywords: Coupled Energy System, Dynamic Simulation, 100 % Renewables, Cost Optimization

*Corresponding author. Tel.: +49-40-42878-2866; fax: +49-40-42878-2967.
E-mail address: c.bode@tuhh.de

10.1016/j.egypro.2018.11.037

1. Introduction

With climate change becoming an ever-increasing concern, it is necessary to reduce CO_2 emissions. A transition to energy systems fully supplied by renewable energies is a viable solution to meet this goal but requires significant changes in the current architecture of the energy sector. Efficiency and costs are the guidelines of this transformation. Because the maximum renewable power generation is limited by the technical potential of the technologies, power has to be used efficiently. Energy still has to be affordable as well, therefore several studies, e.g. [9, 20, 23, 28, 31, 38], have been conducted to find the best configuration of the energy system under certain limits. Most of these studies develop simplified, quasi-stationary models to estimate the need for storage in the future or to optimize cost with Mixed Integer Linear Programming (MILP) but many effects, especially dynamic effects, are neglected. These still have an influence on the system because storage, charging/discharging, networks and transient changes are highly dynamic. These effects have a significant impact on the stability of the system and should be considered, especially in the electric grid.
This paper presents a model with which the dynamic effects in coupled energy systems can be studied. In this case, the model is used to compare different configurations regarding storage and conversion technologies. The transportation sector is neglected due to its uncertain development.

2. Considered system

The considered system represents Germany in the distant future in which the final energy sectors of electricity, heat and gas are supplied by 100 % renewables. Because 2050 is the furthest in the future in most studies, that year is used in most cases as a reference.

2.1. Energy production

The energy production includes only renewables, i.e. wind (on- and offshore), photovoltaics, run-of-river, solar thermal and biogas plants. Other renewable energy sources like geothermal, tidal and wave energy as well as other biomass are not considered due to uncertain future development.
The installed capacity of power-generating renewables in the future, i.e. wind (on- and offshore), photovoltaics and run-of-river plants, depends on the configuration of the overall system and the resulting efficiency. The yearly added capacity is taken from scenario B 2035 in [11] and assumed constant for the following years until the technical potential of each technology (see Table 1) is reached. The technical potential of renewable power generators is 539.3 GW_{el} for Germany. For scenarios that exceed this technical potential, more photovoltaic plants are added because this potential seems to be the most flexible. These scenarios are designed to show the limits of the configurations only and are not considered as feasible options.
To obtain scalable electricity production profiles, the actual feed-in data of the year 2015 of the four transmission

Table 1. Technical potentials and fixed installed capacities for Germany in 2050.

	Technology	Value	Unit
Technical potential:	Wind offshore [23]	45.0	GW_{el}
	Wind onshore [23]	189.0	GW_{el}
	Photovoltaics [23]	300.0	GW_{el}
Installed capacity:	Run-of-river [23]	5.3	GW_{el}
	Solar thermal [23]	85.0	TWh_{th}
	Biogas [23]	96.0	TWh_{NCV}
	Pumped hydro storage [9]	8.6	GW_{el}
		52.1	GWh

system operators [2, 3, 37] is scaled daily with the installed capacity [1]. This eliminates the effect of increasing production with increasing installed power over the year. For run-of-river plants, the curve from [44] is used and scaled as well. To model higher degrees of capacity utilization, those curves are scaled with the full load hours. If the curve exceeds the maximum power after scaling, it is cut at the maximum power and scaled again. This is done iteratively until the desired full load hours are reached.

Renewable heat generation is realized via solar thermal collectors which utilize the radiation from the sun. The amount of generated heat depends on the direct normal irradiance (DNI) and direct horizontal irradiance (DHI). The overall curves for DNI and DHI for Germany are produced by using weighted averages of the curves of weather stations in the six biggest metropolitan regions calculated by [6] with the regarding population [24]. Almost half of the German population lives in those six metropolitan regions so it is assumed to be representative for Germany.

The optimal total solar thermal heat generation was found by [23] to be approximately 50 TWh_{th} on average for households and the commerce, trade and service sector for 80 – 90 % renewable energy in the whole energy system. Scaled up to 100 % renewables, this would lead to approximately 60 TWh_{th}. For industrial purposes, [23] obtained 25 TWh_{th} as an optimum, and [13] states that this is the full potential. Thus, a total production of 85 TWh_{th} solar thermal heat is assumed.

As renewable gas input, biogas is used. An amount of 96 TWh_{NCV} (related to the net calorific value) was found by [23] to be optimal. The costs are considered as per energy specific cost in Table 3.

2.2. Energy demand

The current energy consumption is taken from [10] and split into the end use of electricity, low temperature heat and gas, neglecting the transportation sector. This way, the different final energies can be supplied in various ways with different combinations of conversion and storage technologies.

End use of electricity includes air conditioning, process cooling, mechanical energy (assumed efficiency for oil and gas to mechanical energy: 35 % [44]), information and communication technology, lighting and process heat that is already supplied by electricity. The final low temperature heat consumption consists of space heating and hot water as well as process heat which is supplied by district heating and renewables (assumed conversion efficiencies of oil, gas, district heating, coal, renewables and others in heat: 95 % and electricity to heat with a heat pump: 300 %). The final gas consumption includes the non-energetic use of natural gas [35] and high temperature process heat which is supplied by oil, gas, coal and others so far.

Relative reduction rates were obtained from the target scenario 2050 in [35] and applied to the different categories to calculate the total final energy consumption of electricity (296.1 TWh_{el}), heat (502.9 TWh_{th} of which 288.5 TWh_{th} account for space heating, 170.4 TWh_{th} for hot water generation and 44.0 TWh_{th} for process heat) and gas (295.0 TWh_{NCV}) in the future (see Table 2).

For the final electricity demand curve, the ENTSO-E load profile of 2015 [19] is adjusted using the approach of [17] to obtain an electric demand curve without electricity for heating purposes. A third degree polynomial is used to approximate the relation between the load and the daily mean temperature averaged over the six biggest German metropolitan regions from [15]. The temperature correction adjusts the load profile for temperatures higher than 15 °C. This correction is then scaled linearly to reach the value given in [10].

By using standard load profiles [7, 12], the heat profiles for space heating, hot water and process heat demand are developed. To split up space heating, hot water and process heat demand, the hot water and process heat profile DE_HKO33 is subtracted from each profile, which includes all three demands (DE_HEF33 for one-family houses, DE_HMF33 for apartment buildings, DE_GHD33 for commerce, trade and services). Negative values are set to zero and the profile is scaled to reach the same annual energy. For the industry, the profile DE_GHD33 is used for space heating. Hot water and process heat demand are assumed constant. To determine how much of the total household heat demand is used in one-family houses and how much in apartment buildings, specific heat demands for different ages of the buildings are used from [8] and living spaces of the buildings are taken from [26]. Those two values are combined and total heat demands are calculated and scaled to total values from [10].

Because the non-energetic use of gas and process heat demand occurs mainly in continuous industrial applications and there are no standard load profiles, it is assumed to be a constant load.

Table 2. Final energy demand of Germany in 2050.

Energy sector	Application	Economic Sector	Value	Unit
Electricity			296.1	TWh_{el}
Gas			295.0	TWh_{NCV}
Heat (low temperature)	Space Heating	One family houses	133.4	TWh_{th}
		Apartment buildings	79.0	TWh_{th}
		Commerce, trade and services	41.7	TWh_{th}
		Industry	34.4	TWh_{th}
		Total	288.5	TWh_{th}
	Hot water	One family houses	78.2	TWh_{th}
		Apartment buildings	53.2	TWh_{th}
		Commerce, trade and services	32.0	TWh_{th}
		Industry	7.1	TWh_{th}
		Total	170.4	TWh_{th}
	Process heat	Commerce, trade and services	5.1	TWh_{th}
		Industry	38.9	TWh_{th}
		Total	44.0	TWh_{th}
	Total		502.9	TWh_{th}
Total			1094.0	TWh

2.3. Conversion and storage technologies

The overall system with all considered technologies is shown in Figure 1. For renewable power generation, wind (on- and offshore) as well as run-of-river and photovoltaics plants are considered. Excess power can be stored in pumped hydro storage units, lithium-ion batteries or adiabatic compressed air energy storage units (A-CAES) or it can be consumed in Power-to-Gas (PtG) plants, where electrolyzers produce hydrogen which is transformed into synthetic natural gas (SNG) consuming CO_2 in methanation units. The properties of SNG are similar to natural gas because it consists mainly of methane and small amounts of carbon dioxide and hydrogen. Thus, the present gas infrastructure can be operated with SNG, in contrast to the use of pure hydrogen where a big effort has to be put into adapting the infrastructure. It is assumed that there is sufficient CO_2 in the system to create the desired SNG. The SNG is mixed with biogas and stored in a gas storage. The biogas is assumed to be conditioned and consist of 100 % methane. From there, the gas is supplied for the final gas demand, for re-electrification, employing a gas turbine or combined cycle gas turbine (CCGT), and gas demand for heat production via gas boilers or gas air/water heat pumps. Other heat generators are solar thermal collectors, electric air/water heat pumps and electric boilers. To fit the heat production to the demand, hot water storage tanks are needed.
In general, the energy transmission between the different producers, converters, storage technologies and consumers is assumed ideal, thus there are no transmission losses included in the model.

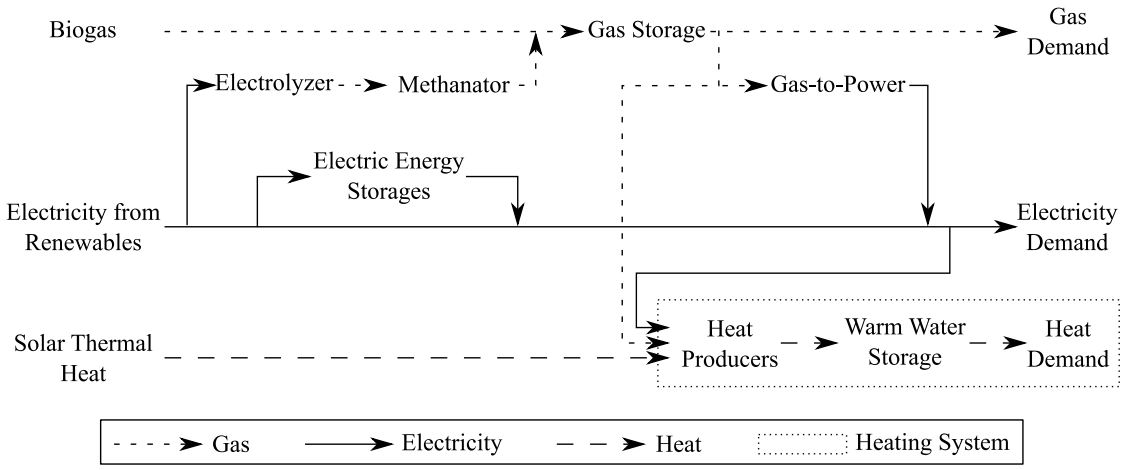

Fig. 1. Overall system.

3. Method

3.1. Approach

The aim is to compare different configurations of the system to supply it with 100 % renewables. Each configuration is tested with different parameter sets and the most cost-efficient solution is used in the overall comparison. Because numerous technologies are considered, there is a wide variety of configurations of the system, i.e. which technologies are used and which sizes are needed. Due to significant computation times with the dynamic models, simplified models are used to perform a parameter study to find and design the most promising configurations. These configurations are then simulated with the more detailed models to obtain more accurate results and compare the different solutions.
Simulations are started with homogeneous configurations, e.g. All-Electric with only electric heat pumps, electric energy storage (EES) technologies and Power-to-Gas for final gas demand or All-Gas with Power-to-Gas, Gas-to-Power, gas boilers, gas heat pumps and no EES technologies except pumped hydro storage. These homogeneous configurations are then mixed with each other to find a cost-efficient solution.
The costs are evaluated using the annuity method after [41] over a period of 20 years with an interest rate of 7 % and no price changes over time. Included are the capital and O&M cost of all components and the variable cost of the incoming biogas. Other variable costs, e.g. of the electricity, are not considered because the electricity is consumed within the system. Costs for power exchange with the surrounding grid are neglected.

3.2. Models

The models used are taken from or based on the open-source Modelica® library TransiEnt Library [4, 5, 22]. Modelica® is an object-oriented, equation-based language which allows for dynamic simulations of multi-domain systems [27]. Therefore, the TransiEnt Library is suitable to simulate coupled energy systems with different levels of detail.
To make the analysis faster, all used models have a simplified, i.e. quasi-stationary, representation which is used for the rough design of the components. Those models are solved in 900s time steps because this is the time step of the renewable production data. Due to these large time steps, load gradients, time constants and start-up times are neglected.
All technical and economical parameters of the components are summarized in Tables 3 and 4.
The heating system is shown in more detail in Figure 2. This system is a simplification of the actual heating system. All consumers utilizing the same heat producer (gas boiler, electric heat pump or gas heat pump) are lumped together and take heat from one large hot water storage tank. The respective lumped heat producers, including a proportional

Table 3. Technical and economical parameters of the system.

Wind offshore		
Capital cost [23]	2251	€/kW$_{el}$
Yearly O&M cost [23]	68.2	€/kW$_{el}$
Lifetime [23]	20	a
Full load hours [33]	4307	h
Wind onshore		
Capital cost [23]	1167	€/kW$_{el}$
Yearly O&M cost [23]	39.7	€/kW$_{el}$
Lifetime [23]	22.5	a
Full load hours [23]	2250	h
Photovoltaics		
Capital cost [23]	571	€/kW$_{el}$
Yearly O&M cost [23]	11.2	€/kW$_{el}$
Lifetime [23]	30	a
Full load hours [23]	950	h
Run-of-river		
Capital cost [23]	1600	€/kW$_{el}$
Yearly O&M cost [23]	32.0	€/kW$_{el}$
Lifetime [23]	50	a
Full load hours [33]	3989	h
Solar thermal collectors		
Capital cost [23]	162	€/m^2
Yearly O&M cost [23]	2.1	€/m^2
Lifetime [23]	30	a
Biogas		
Variable cost [13]	50	€/MWh$_{NCV}$
Electrolyzer		
Capital cost [13]	200	€/kW$_{el}$
Yearly O&M cost [13]	8.0	€/kW$_{el}$
Lifetime [13]	18.5	a
Efficiency rel. to NCV [28]	75	%
Time constant (assumption)	10	s
Methanation unit		
Capital cost related to electrolyzer power [13]	800	€/kW$_{el}$
Yearly O&M cost related to electrolyzer power [13]	20.0	€/kW$_{el}$
Lifetime [13]	25	a
Number of control volumes	5	-
Feed/cooling temperature [34]	285	°C
Tube diameter [34]	0.02	m
Tube length [34]	6.94	m
Equivalent particle diameter [34]	0.003	m
Bed porosity [34]	0.4	-
Bed density [34]	2350	kg/m^3
Specific heat capacity of catalyst (assumption)	790	J/(kg K)
Particle conductivity (assumption)	50	W/(m K)

Combined cycle gas turbine		
Capital cost [21]	700	€/kW$_{el}$
Yearly O&M cost [21]	21.0	€/kW$_{el}$
Lifetime [21]	32.5	a
Efficiency [21]	63.5	%
Relative minimum power [21]	37.5	%$P_{el,n}$
Max. load change gradient [21]	10.5	%$P_{el,n}$/min
Time constant (assumption)	6	min
Start-up time [21]	19.5	min
Gas turbine		
Capital cost [21]	375	€/kW$_{el}$
Yearly O&M cost [21]	13.1	€/kW$_{el}$
Lifetime [21]	50	a
Efficiency [21]	46	%
Relative minimum power [21]	14	%$P_{el,n}$
Max. load change gradient [21]	100	%$P_{el,n}$/min
Time constant (assumption)	0.63	min
Start-up time [21]	5	min
Electric heat pump		
Capital cost [23]	956	€/kW$_{th}$
Yearly O&M cost [23]	33.5	€/kW$_{th}$
Lifetime [23]	20	a
COP [23]	3.47	-
Electric boiler		
Capital cost [18]	70	€/kW$_{th}$
Yearly O&M cost [18]	1.4	€/kW$_{th}$
Lifetime [18]	15	a
Efficiency [20]	99	%
Gas heat pump		
Capital cost [23]	800	€/kW$_{th}$
Yearly O&M cost [23]	12.0	€/kW$_{th}$
Lifetime [23]	20	a
COP [23]	1.38	-
Gas boiler		
Capital cost [13]	652	€/kW$_{th}$
Yearly O&M cost [13]	18.3	€/kW$_{th}$
Lifetime [23]	20	a
Efficiency [13]	95	%
Pumped hydro storage		
Capital cost [18]	850	€/kW$_{el}$
	50	€/kWh
Yearly O&M cost [18]	10.2	€/kW$_{el}$
	0.6	€/kWh
Lifetime [18]	40	a
Charging efficiency [18]	88	%
Discharging efficiency [18]	89	%
Min./max. SOC [18]	0-100	%
Max. load change gradient [40]	60	%$P_{el,n}$/min

Table 4. Technical and economical parameters of the system, continued.

A-CAES		
Capital cost [18]	650	€/kW$_{el}$
	23	€/kWh
Yearly O&M cost [18]	6.5	€/kW$_{el}$
Lifetime [18]	40	a
Charging efficiency [18]	87	%
Discharging efficiency [18]	78	%
Min./max. SOC [18]	60-100	%
Max. load change gradient [43]	10	%$P_{el,n}$/min
Lithium-ion battery		
Capital cost [18]	45	€/kW$_{el}$
	150	€/kWh$_{el}$
Yearly O&M cost [18]	0.5	€/kW$_{el}$
	1.5	€/kWh$_{el}$
Lifetime [18]	25	a
Charging efficiency [18]	95	%
Disharging efficiency [18]	95	%
Max. load change gradient (assumption)	60000	%$P_{el,n}$/min
Min./max. SOC [18]	0-100	%
Self-discharge rate [43]	2	%/month

Hot water storage		
Capital cost [23]	1040	€/m^3
Yearly O&M cost [23]	1.3	€/m^3
Lifetime [23]	20	a
Height (assumption)	2	m
Diameter (assumption)	1	m
Number of control volumes	10	-
Coefficient of heat transmission through storage wall (assumption)	0.5	W/(m^2 K)
Conductivity of water	0.6	W/(m K)
Density of water	1000	kg/m^3
Specific heat capacity of water	4185	J/(kg K)
Gas storage		
Capital cost [36]	6.24	€/kg
Yearly O&M cost [36]	0.12	€/kg
Lifetime [36]	30	a

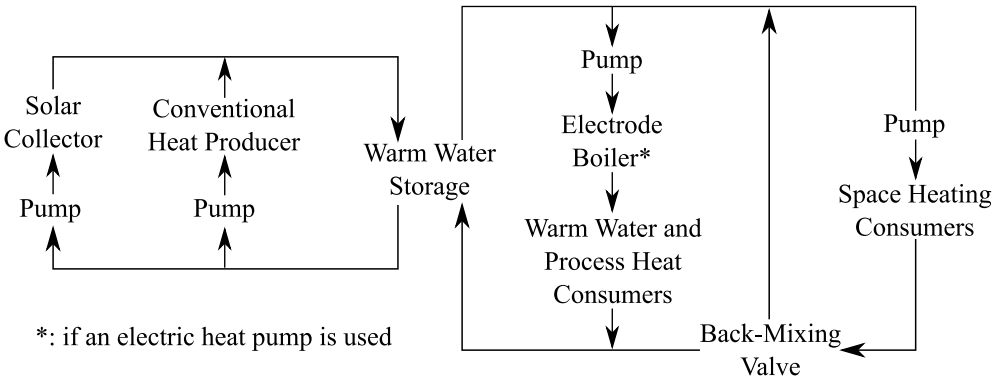

Fig. 2. Heating system.

share of lumped solar thermal collectors, charge the storage to supply the consumers. It has an equivalent surface area and volume to several small hot water storage tanks. This way, the heat losses are the same. On the consumer side, heat for space heating is separated from heat for hot water and process heat. For space heating a heating curve with a maximum supply temperature of 45 °C and a maximum return temperature of 35 °C at −12 °C ambient temperature is used. Above 20 °C ambient temperature, supply and return temperature equal 20 °C. For the hot water and process heat side, 60 °C supply and 15 °C return temperature are assumed. When an electric heat pump is designated as the main heat producer, an electric boiler raises the temperature to 60 °C so that the output temperature of the heat pump is lower, for efficient operation.

3.2.1. Electric energy storage technologies

All EES models are based on the same principles. The energy content has to be between minimum and maximum values and charging and discharging powers are limited to maximum powers. Constant charging and discharging efficiencies can be given as well as different stationary loss models. For the pumped hydro storage and A-CAES models, no stationary losses are considered. For the lithium-ion battery, the loss is calculated with a constant self-discharge rate and the current energy within the battery.

3.2.2. Power-to-Gas

The Power-to-Gas station consists of two main components: the electrolyzer, which produces hydrogen, and the methanation unit which uses this hydrogen and added carbon dioxide to produce SNG.
The electrolyzer is modeled with 1st-order dynamics and an efficiency curve of a real electrolyzer [25]. Output pressure and temperature are set constant.
The model of the methanation unit represents a cooled fixed-bed reactor which contains CO_2 methanation reaction kinetics in a desired number of control volumes including mass and energy balances in axial direction as well as heat transfer from [34]. Pressure loss, effectiveness factors of the reaction and density are assumed constant. The hydrogen is mixed with a stoichiometric amount of CO_2, preheated, converted mostly to methane and steam in the methanation unit, cooled to a constant temperature and dried completely to zero water content. No minimum load is considered so no buffer storage is necessary between the electrolyzer and methanation unit.

3.2.3. Gas storage

The gas storage model consists of one volume with mass balances (single components and complete mixture) and the mass specific costs of the gas storage are calculated based on a 500 000 m^3 green field cavern and cost values from [36].

3.2.4. Gas-to-Power

For re-electrification of the SNG, gas turbines or combined cycle gas turbines can be used. The output power is set according to minimum and maximum power values as well as a maximum gradient and 1st-order dynamics. During start-up time, the electric output remains zero. The gas demand is calculated with the efficiency at the current electric power using a nominal efficiency and a part load efficiency curve from [14]. To be able to cover small residual loads as well, it is assumed that the plant consists of several small plants where the smallest unit has a power of 50 MW_{el} for gas turbines and 100 MW_{el} for combined cycle gas turbines. These small units are lumped together into one large unit with one efficiency curve and the respective low minimal load of one small unit.

3.2.5. Heat producers

The conventional heat producers (gas boilers, electric air/water heat pumps, gas air/water heat pumps and electric boilers) produce given heat flows and the gas or electric demand of the heat producer is calculated using a constant efficiency for the gas boiler as well as the electric boiler and COP curves for the heat pumps where the COP is calculated depending on the temperature difference between heat source (ambient air) and sink (heating water) [30].
The renewable heat producer model (solar thermal collector) contains an energy balance with a heat capacity from [29], a radiation model from [16] and a solar time model from [32]. Longitude and latitude for the solar time model are calculated by using a weighted average of the coordinates of the weather stations with the population of the respective metropolitan region. The data of the solar collector is taken from a data sheet of a real collector [42].

3.2.6. Hot water storage

The hot water storage is modeled with a desired number of axially distributed control volumes which contain water with constant properties. The water can flow from one volume to the adjacent ones and each volume can exchange heat with the surroundings, i.e. with neighboring control volumes by diffusion and buoyancy and with the ambient air through the wall of the storage. Diffusion is calculated with a constant thermal conductivity of the water and buoyancy is modeled with a time constant as in [39].

3.2.7. Control strategy

The EES and conversion technologies (electrolyzer and methanation unit as well as Gas-to-Power plant) are controlled so that the electricity demand is always met. To achieve efficient operation, the storage units are sorted by efficiency and then charged and discharged in this order. So, if there is a negative residual load, the most efficient storage is charged. The actual charging power of the storage unit is subtracted from the residual load and the remaining power is used to charge the next unit. This way, load gradients and maximum powers of the storage units are taken into account and in an attempt to avoid residual loads. If a storage unit is full or empty, it cannot be charged or discharged respectively and the next unit is used. The considered storage units are charged/discharged in one of the following two orders: lithium-ion battery, pumped hydro storage, A-CAES, electrolyzer/Gas-to-Power, or pumped hydro storage, lithium-ion battery, A-CAES, electrolyzer/Gas-to-Power. The latter takes into account that the efficiency of the lithium-ion battery can be lower than that of the pumped hydro storage due to stationary losses over time.

Due to storage components generating frequent events upon each change of state between full (state of charge (SOC) = 1) and not full (SOC < 1) or empty (SOC = 0) and not empty (SOC > 0), hystereses between SOC = 1 and SOC = 0.999 as well as between SOC = 0.001 and SOC = 0 are used to avoid long simulation times. However, this slightly decreases the usable energy capacity of the storage.

The aim of the control of the heating system is to cover the heat demand at any time. This is ensured by keeping the temperature at the top of the hot water storage 1 K above the maximum supply temperature for space heating in the case of an electric heat pump or at 60 °C for the gas boiler and gas heat pump by setting an appropriate heat flow. It is assumed that all conventional heat producers in the system are only turned on at nominal heat flow and turned off when a target temperature is reached. Because all conventional heat producers are lumped together here, the switching of individual heat producers is not seen in the overall produced heat flow curve and the lumped model is one equivalent conventional heat producer with a constant load-independent efficiency instead.

The target outlet temperature of the electric heat pump is set to 5 K above the maximum supply temperature for space heating and to 75 °C for gas boiler, gas heat pump and solar thermal collectors. The pumps in the respective branch are controlled with these temperatures.

On the consumer side, the space heating supply temperature is reached by back-mixing of return water. The return temperature is held by controlling the pump mass flow. The latter is done in the hot water and process heat branch as well. When an electric heat pump is used, the electric boiler raises the temperature to 60 °C before the consumer.

4. Design of components

4.1. Heating System

The heating system is simulated with one equivalent conventional heat producer and solar thermal collectors to supply the demanded heat. Different conventional heat producers can then be combined by linearly scaling all components.

The required area of the solar thermal collectors is designed to meet the annual heat demands. For the conventional heat producers, the nominal heat flow is set to the maximum heat flow in that year. The volume of the hot water storage is calculated to be large enough such that the temperature at the bottom approaches close to the temperature at the top but never fully reaches it. The resulting component sizes are shown in Table 5.

4.2. Overall System

In the system, the capacities and maximum electric powers of the EES units and sizes of electrolyzer, methanation unit, gas storage and Gas-to-Power units are chosen so that all demands are met. The state of charge of all storage units including the gas storage is the same at the beginning and end of the year to allow for periodic operation. The size of the equivalent pumped hydro storage unit (52.1 GWh, 8.6 GW_{el} for Germany) is assumed constant in the long term, taken from [9] for 2050. Every configuration contains these and the installed power and capacity are not varied. Different sizes of lithium-ion batteries and A-CAES are compared, and the storage sizes are designed with the simplified models for the discrete energy capacities in the interval $1, 2 \ldots 9 \cdot 10^{10,11 \ldots 16}$ which results in 63 possible sizes for

Table 5. Design parameters of the heating systems.

		Heat producer power in GW_{th}	Hot water storage volume in mil. m^3	Solar thermal collector area in mil. m^2
Electric heat pump and electric boiler	El. heat pump:	147.5	45.95	327.1
	Electric boiler:	11.4		
Gas boiler		156.3	35.01	329.5
Gas heat pump		156.3	35.01	329.5

Table 6. Overview of the abbreviations of the configurations.

EHP	GB	GHP	PHS	Li	CAES	PtG	GT	CCGT
Electric heat pump	Gas boiler	Gas heat pump	Pumped hydro storage	Lithium-ion battery	A-CAES	Power-to-Gas	Gas turbine	Combined cycle gas turbine

each storage. Also, different charging times are considered for both storage technologies. Charging times are determined by dividing energy capacity by maximum charging power and the times used for this study are ten minutes, one hour, six hours, one day, three days and one week. For the complex models, the most significant configurations were designed in detail to ensure that the best solution in this set of parameter combinations was found.
Small residual loads, which result from minimal loads of the Gas-to-Power units or time constants of the components, are tolerated and given to or taken from the surrounding grid. Curtailment of the renewables is not considered, thus all generated energy is stored in the storage units.

5. Results

The configurations are named in the following pattern: "A_B_C". "A" stands for the heating system, "B" for the storage system and "C" for the Gas-to-Power plant using the abbreviations given in Table 6. For the storage system, the different technologies are utilized in the given order. Table 7 gives an overview of the considered configurations and the corresponding technologies. Configurations that did not yield viable results are not listed here.
The configurations are sorted into five categories:

- All-Electric: All services are supplied by electricity using pumped hydro storage and one other EES technology, Power-to-Gas is only operated for the final gas demand.
- All-Gas: All services are supplied using gas, there are no EES units considered except pumped hydro storage.
- All-Gas with electric and gas heat pumps: Extension of All-Gas but electric heat pumps are employed combined with gas heat pumps.
- Li or A-CAES and Gas-to-Power: Only electric heat pumps are used to supply heat. Pumped hydro storage and one additional EES and Gas-to-Power are considered.
- Li, A-CAES and Gas-to-Power: Extension of the former category but a lithium-ion battery and an A-CAES are employed combined with pumped hydro storage and Gas-to-Power.

Table 7. Considered configurations.

Category	Configuration	EHP	GB	GHP	PHS	Li	CAES	PtG	GT	CCGT
All-Electric	EHP_LiPHSPtG	X			X	X		X		
	EHP_PHSLiPtG	X			X	X		X		
	EHP_PHSCAESPtG	X			X		X	X		
All-Gas	GB_PHSPtG_CCGT		X		X			X		X
	GHP_PHSPtG_CCGT			X	X			X		X
	GB_PHSPtG_GT		X		X			X	X	
	GHP_PHSPtG_GT			X	X			X	X	
All-Gas with electric and gas heat pumps	GHPEHP_PHSPtG_CCGT	X		X	X			X		X
	GHPEHP_PHSPtG_GT	X		X	X			X	X	
Li or A-CAES and Gas-to-Power	EHP_LiPHSPtG_CCGT	X			X	X		X		X
	EHP_PHSLiPtG_CCGT	X			X	X		X		X
	EHP_PHSCAESPtG_CCGT	X			X		X	X		X
Li, A-CAES and Gas-to-Power	EHP_LiPHSCAESPtG_CCGT	X			X	X	X	X		X
	EHP_PHSLiCAESPtG_CCGT	X			X	X	X	X		X

5.1. All-Electric

First, the extreme scenario of a system, which is mainly based on electricity ("All-Electric"), is designed. Power-to-Gas is only operated to supply the final gas demand and all other demands are covered using electricity (electric heat pumps, EES units). Three configurations are considered: One employing a lithium-ion battery, which is charged and discharged before the pumped hydro storage, (EHP_LiPHSPtG), one in which the lithium-ion battery is charged and discharged after the pumped hydro storage, (EHP_PHSLiPtG), and one considering an A-CAES after the pumped hydro storage (EHP_PHSCAESPtG). The energy capacity and maximum power were minimized but chosen to be sufficiently large so that no re-electrification is necessary. Combinations of a battery and an A-CAES have been tested as well but a more cost-efficient configuration could not be found in the simplified simulations. The design parameters and most important results are shown in Table 8.

The results of the dynamic and the simplified simulations fit quite well. There are small deviations in the required sizes of the components and the total costs which mainly results from the more detailed design of the storage sizes in the dynamic simulations.

Charging the battery before the pumped hydro storage leads to a higher battery efficiency due to less stationary losses, and thus, lowers the cost in the dynamic simulations. The cheapest solution is the usage of an A-CAES (EHP_PHSCAES_PtG). Using a battery is more efficient despite the self-discharge rate, so less renewable electricity producers are needed, and the required electrolyzer is smaller. However, the batteries are expensive, with annuities of 279.86 bil. € and 280.86 bil. €, which is 72.28 % and 72.32 % of the total cost, compared to the A-CAES with 134.85 bil. € (55.06 %).

Table 8. Results of the All-Electric configurations.

Simulations	EHP_LiPHSPtG Simplified	EHP_LiPHSPtG Dynamic	EHP_PHSLiPtG Simplified	EHP_PHSLiPtG Dynamic	EHP_PHSCAESPtG Simplified	EHP_PHSCAESPtG Dynamic
Storage capacity in PJ	Li: 67.68	Li: 67.39	Li: 67.93	Li: 67.63	A-CAES: 219.90	A-CAES: 219.10
Storage charging power in GW_{el}	96.61	96.64	96.61	96.64	96.61	96.64
Renewable electric power in GW_{el}	408.6	411.7	410.0	413.2	430.0	433.3
Electrolyzer power in GW_{el}	224.7	226.7	224.8	227.6	235.2	240.7
Gas storage in mil. kg	2908	3010	2916	3019	3287	3394
Battery efficiency in %	85.78	85.78	85.31	85.31	-	-
Power-to-Gas efficiency related to NCV in %	66.55	66.65	66.52	66.63	66.53	66.59
Annuity in bil. €	387.96	387.19	389.10	388.35	244.65	244.92

Table 9. Results of the All-Gas configurations.

Simulations	GB_PHSPtG_CCGT Simplified	GB_PHSPtG_CCGT Dynamic	GHP_PHSPtG_CCGT Simplified	GHP_PHSPtG_CCGT Dynamic	GB_PHSPtG_GT Simplified	GB_PHSPtG_GT Dynamic	GHP_PHSPtG_GT Simplified	GHP_PHSPtG_GT Dynamic
Renewable electric power in GW_{el}	953.8	954.7	833.8	835.0	969.9	971.2	850.0	851.8
Electrolyzer power in GW_{el}	593.0	587.9	510.9	507.8	604.1	598.9	522.1	519.0
Gas-to-Power power in GW_{el}	34.25	33.84	34.25	33.85	34.25	33.84	34.25	33.85
Gas storage in mil. kg	15550	15980	12777	13131	15884	16325	13120	13485
Power-to-Gas efficiency related to NCV in %	65.47	65.52	65.75	65.80	65.44	65.49	65.71	65.76
Gas-to-Power efficiency related to NCV in %	54.05	54.34	54.10	54.38	33.54	32.09	31.93	32.14
Annuity in bil. €	175.73	175.60	160.31	160.33	176.58	176.50	161.21	161.26

5.2. All-Gas

Second, the other extreme "All-Gas" is considered: All negative residual loads after the pumped hydro storage are consumed by the electrolyzer and the SNG supplies the heat sector using gas boilers or gas heat pumps and the electricity sector in times of positive residual loads via re-electrification. The following configurations are considered: Exclusively gas boilers in the heat sector and CCGT for re-electrification (GB_PHSPtG_CCGT), gas heat pumps and CCGT (GHP_PHSPtG_CCGT), gas boilers and gas turbines (GB_PHSPtG_GT) and gas heat pumps and gas turbines (GHP_PHSPtG_GT). The design parameters and important results are summarized in Table 9. The results of the simplified and dynamic simulations differ slightly in components sizes but fit very well in regard of the cost.
Configurations with gas heat pumps and/or CCGT are more economic than those with gas boilers and/or gas turbines because the higher efficiency of the gas heat pumps and CCGTs leads to a decrease in needed renewable power generation and electrolyzer power as well as smaller gas storage volumes.

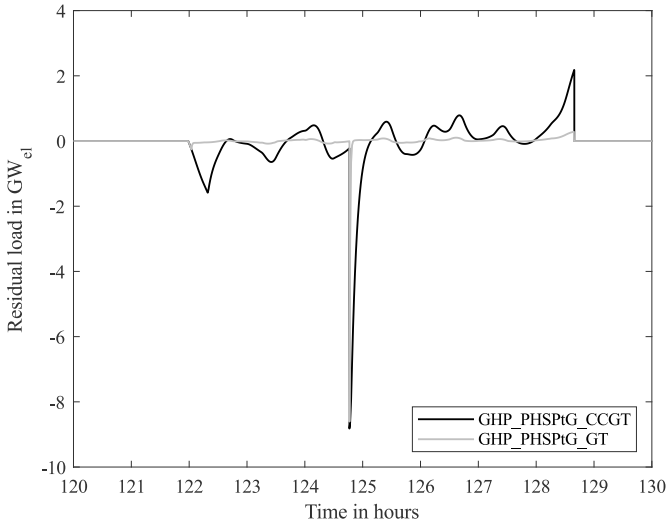

Fig. 3. Residual loads to and from the surrounding grid for GHP_PHSPtG_CCGT and GHP_PHSPtG_GT.

Even though these configurations are much cheaper than the All-Electric scenarios, the required renewable power generation is much higher and even exceeds its technical potential. The conversion steps from electricity to SNG and then to power or heat are much less efficient than the direct usage of electricity in electric heat pumps. The most efficient All-Gas (GHP_PHSPtG_CCGT) still requires 401.7 GW_{el} more power from renewables than the least efficient All-Electric scenario (EHP_PHSCAESPtG), exceeding the technical potential by 295.7 GW_{el} or 54.8 %.
There is also a significant difference in the residual loads that are exchanged with the surrounding grid. In the All-Electric scenarios with a lithium-ion battery, only short peaks occur due to the maximum load gradients because of the fast response time of the battery. The EHP_LiPHSPtG scenario only exhibits a longer peak on that one occasion when the battery is empty and the pumped hydro storage is used as the main supply instead, since the pumped hydro storage has a lower load change gradient than the battery. In the All-Gas scenarios, more power is given to or taken from the surrounding grid because the start-up times and time constants lead to a delay between supply and demand and thus to residual loads. In Figure 3 the differences between the gas turbine and CCGT can be seen: The peaks and delays are longer when a CCGT is used.

5.3. All-Gas with electric and gas heat pumps

Because the EES technologies are expensive but the direct use of the electricity in the electric heat pumps is highly efficient, All-Electric and All-Gas are combined so that no EES units except pumped hydro storage are used, and electric heat pumps and gas heat pumps are mixed. Gas boilers are omitted because they are not cost-efficient. However, CCGT (GHPEHP_PHSPtG_CCGT) and gas turbines (GHPEHP_PHSPtG_GT) are still both considered because gas turbines may be cost-efficient in this case.
Figure 4 shows that the use of electric heat pumps decreases the cost of the system and for configurations with CCGT the decrease is even greater due to the increased need for re-electrification and therefore greater effect of the increased efficiency of the CCGT. The minimum costs are reached at 100 % electric heat pumps in both cases but using a CCGT is still most cost-efficient.
In Figure 5 the necessary renewable power for each configuration is shown. It is evident that almost no configuration except those with CCGT and 100 % electric heat pumps stay within the technical potential of renewables.

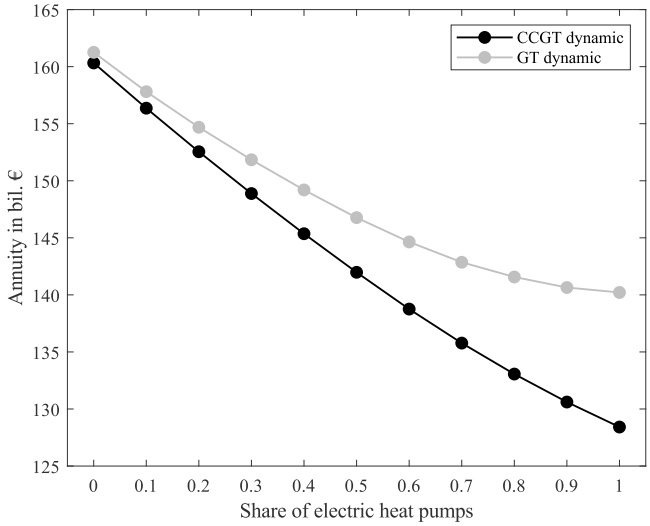

Fig. 4. Cost over share of electric heat pumps for GHPEHP_PHSPtG_CCGT and GHPEHP_PHSPtG_GT.

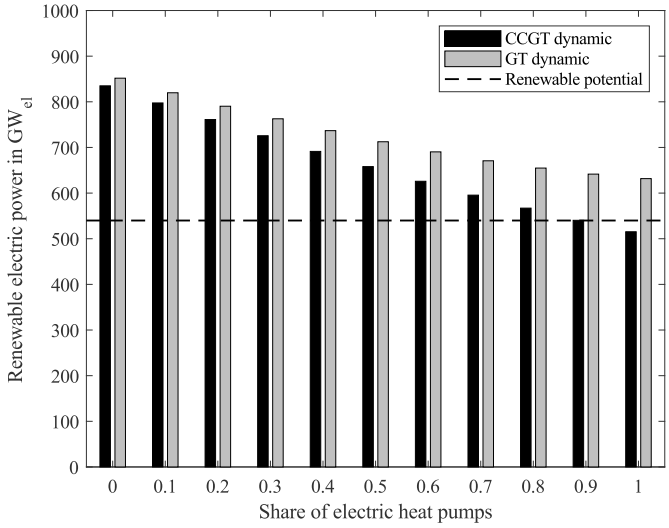

Fig. 5. Required renewable power generators for GHPEHP_PHSPtG_CCGT and GHPEHP_PHSPtG_GT.

5.4. Lithium-ion battery or A-CAES and Gas-to-Power

In the next step, one EES is added to the configuration with 100 % electric heat pumps and CCGT because this was the most economical solution so far. The three options EHP_LiPHSPtG_CCGT, EHP_PHSLiPtG_CCGT and EHP_PHSCAESPtG_CCGT are designed for various energy capacities in the interval of $10^{10} \ldots 9 \cdot 10^{16}$ and different charging times from ten minutes to one week.

In the simplified simulations, the configurations with charging times of one and six hours for lithium-ion batteries and one and three days for A-CAES are the most economic. These configurations are thus designed in more detail using the dynamic simulations and the results are shown in Tables 10 and 11.

Here, the dynamic and simplified results are very similar again but there are still deviations. Within each configuration,

Table 10. Results of the configurations with lithium-ion battery and Gas-to-Power.

Charging times	EHP_LiPHSPtG_CCGT				EHP_PHSLiPtG_CCGT			
	1 hour		6 hours		1 hour		6 hours	
Simulations	Simplified	Dynamic	Simplified	Dynamic	Simplified	Dynamic	Simplified	Dynamic
Storage capacity in TJ	300	300	500	500	300	300	500	500
Renewable electric power in GW_{el}	494.7	494.3	488.6	490.1	494.0	493.8	488.9	490.6
Electrolyzer power in GW_{el}	280.5	279.8	276.6	276.9	280.1	279.4	276.8	277.2
Gas-to-Power power in GW_{el}	96.61	96.44	96.61	96.44	96.61	96.44	96.61	96.44
Gas storage in mil. kg	4728	4836	4696	4827	4721	4836	4705	4838
Battery efficiency in %	90.14	90.14	90.12	90.12	90.10	90.10	90.07	90.07
Power-to-Gas efficiency related to NCV in %	66.55	66.62	66.46	66.52	66.55	66.62	66.46	66.52
Gas-to-Power efficiency related to NCV in %	54.24	54.32	54.34	54.80	54.51	54.59	54.45	54.91
Annuity in bil. €	127.44	127.41	127.28	127.47	127.36	127.35	127.32	127.53

Table 11. Results of the configurations with A-CAES and Gas-to-Power.

Charging times	EHP_PHSCAESPtG_CCGT			
	1 day		3 days	
Simulations	Simplified	Dynamic	Simplified	Dynamic
Storage capacity in TJ	1000	1000	200	100
Renewable electric power in GW_{el}	500.8	502.7	512.3	514.7
Electrolyzer power in GW_{el}	284.5	285.3	292.0	293.4
Gas-to-Power power in GW_{el}	96.61	96.44	96.60	96.44
Gas storage in mil. kg	4795	4943	4920	5083
Power-to-Gas efficiency related to NCV in %	66.42	66.48	66.36	66.40
Gas-to-Power efficiency related to NCV in %	53.75	53.84	53.12	53.20
Annuity in bil. €	127.86	128.13	128.15	128.43

i.e. each combination of storage type and charging time, the same storage size was found to be the cheapest except for EHP_PHSCAESPtG_CCGT with a charging time of three days where a smaller storage was the best solution.
The configurations, where the lithium-ion battery is charged before the pumped hydro storage, have a higher battery efficiency. Compared to EHP_LiPHSPtG and EHP_PHSLiPtG, where the battery was the only storage technology, the efficiency of the battery is higher, with 90.07-90.14 % efficiency compared to 85.31-85.78 % due to less operation at high capacity and thus lower stationary losses. Using an A-CAES leads to higher overall cost because the efficiency of the storage is so much lower and is not outweighed by its lower cost.
The best parameter set in the simplified simulations was EHP_LiPHSPtG_CCGT with a charging time of six hours but in the dynamic simulations EHP_PHSLiPtG_CCGT with a charging time of one hour was found to be cheaper. This

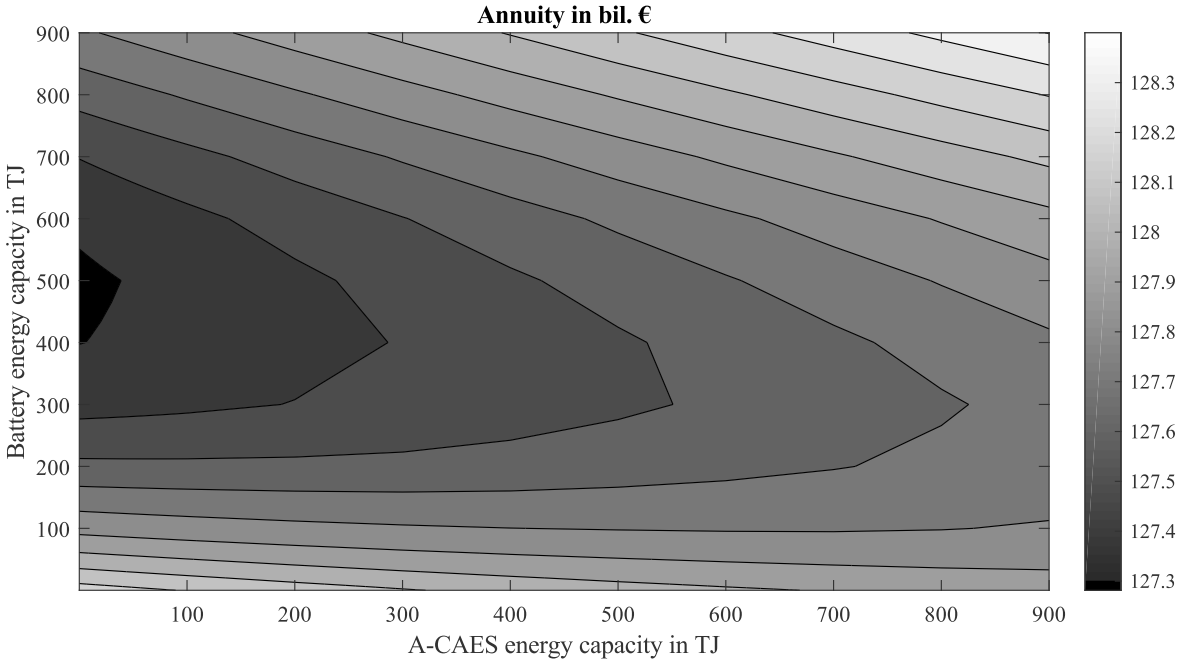

Fig. 6. Variation of lithium-ion battery and A-CAES sizes with charging times of six hours (battery) and one day (A-CAES).

is due to the differences in efficiencies of the other components. In the dynamic simulations, the configurations with charging times of one hour become more efficient and those with charging times of six hours become less efficient compared to the simplified simulations. However, the cost of the different configurations are very similar so the results are very sensitive.

5.5. Lithium-ion battery, A-CAES and Gas-to-Power

In the last configuration, a lithium-ion battery is combined with an A-CAES to see if there is an advantage in combining the A-CAES, with cheaper large storage volumes and no self-discharge rate, with the high storage efficiency of the battery.
The same variations have been made for both storage technologies combined as they were for one EES. However, no advantage has been found. Every variation leads to the result that using only one storage with its most economic charging time from the previous section is the best option. As an example, Figure 6 shows this behavior for one combination. It is evident that the lowest cost can be reached with a lithium-ion battery with a capacity around 500 TJ and no A-CAES.
Based on the similarity between the simple and complex models of the best solutions in the previous sections, it is assumed that no better solution will be found with the dynamic simulations. Thus, no further simulations are conducted.

5.6. Summary

The costs of the most important configurations are shown in Figure 7. The greatest differences between the configurations can be seen in the sum and the shares of the different parts. All-Electric has the highest cost with the most significant cost being that of the EES. The costs are reduced when smaller storage or EES is used due to the comparatively cheaper Power-to-Gas-to-Power technologies. With more Power-to-Gas and Gas-to-Power, more renewable power generators are needed because of the lower efficiency. However, it is still cheaper. The most economical configuration is the one that utilizes a lithium-ion battery with a charging time of one hour which is charged and discharged at a lower priority than the pumped hydro storage and the Power-to-Gas plant with a total cost of 127.35 bil. €.

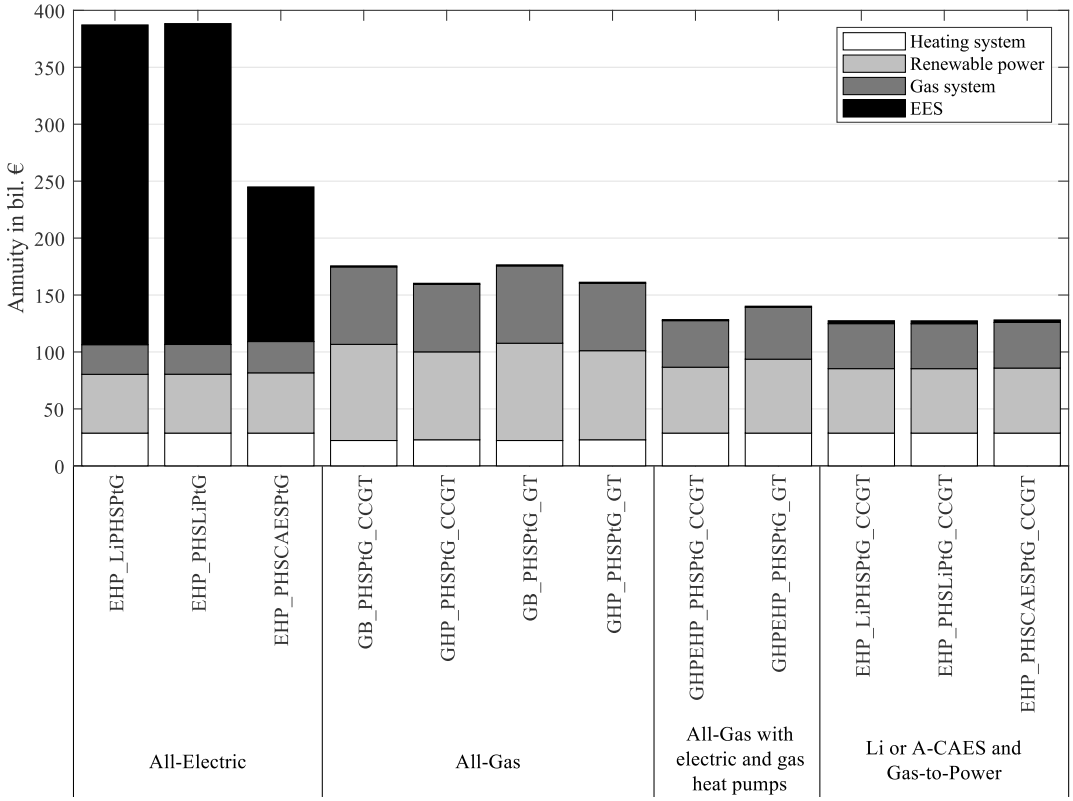

Fig. 7. Summary of the most important configurations and their costs.

6. Conclusions

A comparison of different configurations of a coupled energy system supplying final energy demands of electricity, heat and gas with exclusively renewable energies has been presented using simplified, quasi-stationary and detailed, dynamic models. It has been proved that homogeneous configurations, based entirely on electricity or gas, are more expensive than mixed configurations. The technical potential of renewable power generators does not suffice to supply the whole demand, especially when a significant proportion of Power-to-Gas and Gas-to-Power/Heat technologies is in use, whereas using no Power-to-Gas and Gas-to-Power/Heat requires large and expensive, but efficient, EES units. A combination of Power-to-Gas with a CCGT, only electric heat pumps for the low temperature heat supply and an appropriately sized lithium-ion battery, which is charged at a lower priority than a pumped hydro storage, has the best cost performance. Adding an A-CAES does not further reduce the cost. An important note is that several configurations had only slightly differing cost which means that the optimal solution is highly sensitive to the input parameters, e.g. cost, which was also observed by [23].

A difference has been found in the electric residual loads that are supplied to or taken from the surrounding grid depending on the configuration. If gas turbines or CCGTs are used, there will be significant residual loads due to start-up times, load gradients and especially minimal loads throughout the whole year. In All-Electric configurations, only smaller residual loads remain during most of the year since there are no Gas-to-Power units, but high peaks can still occur, mainly because of the limited load gradient of the pumped hydro storage. Smaller decentral units, e.g. small-scale combined heat and power units, which were not considered here, will reduce those residual loads caused by the gas turbines and CCGT even more. These differences influence the resilience of the electric grid and, thus, the whole system. This will be studied in detail in future work because it is an important aspect of energy supply that will influence the architecture of the system.

The simplified simulations are a useful tool for quickly evaluating various configurations of an overall system, however they do not take into account important dynamic effects. If the resilience of a system is to be examined, dynamic simulations will become inevitable.

References

[1] 50Hertz Transmission GmbH, Amprion GmbH, TransnetBW GmbH, TenneT TSO GmbH, 2016. EEG-Anlagenstammdaten. URL: https://www.netztransparenz.de/EEG/Anlagenstammdaten.

[2] 50Hertz Transmission GmbH, Amprion GmbH, TransnetBW GmbH, TenneT TSO GmbH, 2017a. Solarenergie Hochrechnung. URL: https://www.netztransparenz.de/Weitere-Veroeffentlichungen/Solarenergie-Hochrechnung.

[3] 50Hertz Transmission GmbH, Amprion GmbH, TransnetBW GmbH, TenneT TSO GmbH, 2017b. Windenergie Hochrechnung. URL: https://www.netztransparenz.de/Weitere-Veroeffentlichungen/Windenergie-Hochrechnung.

[4] Andresen, L., Dubucq, P., Peniche, R., Ackermann, G., Kather, A., Schmitz, G., 2015. Status of the TransiEnt Library: Transient simulation of coupled energy networks with high share of renewable energy, in: Proceedings of the 11th International Modelica Conference, Versailles. pp. 695–705. doi:10.3384/ecp15118695.

[5] Andresen, L., Dubucq, P., Peniche Garcia, R., Ackermann, G., Kather, A., Schmitz, G., 2017. Transientes Verhalten gekoppelter Energienetze mit hohem Anteil Erneuerbarer Energien: Abschlussbericht des Verbundvorhabens. Technical Report. Hamburg.

[6] Baldauf, M., Förstner, J., Klink, S., Reinhardt, T., Schraff, C., Seifert, A., Stephan, K., 2014. Kurze Beschreibung des Lokal-Modells Kürzestfrist COSMO-DE (LMK) und seiner Datenbanken auf dem Datenserver des DWD. Technical Report. Offenbach.

[7] BDEW, VKU, GEODE, 2016. BDEW / VKU / GEODE- Leitfaden. Abwicklung von Standardlastprofilen Gas. Technical Report. Berlin.

[8] Beer, M.G., 2012. Regionalisiertes Energiemodell zur Analyse der flexiblen Betriebsweise von Kraft-Wärme-Kopplungsanlagen. Phd thesis. Technische Universität München.

[9] Benndorf, R., Bernicke, M., Bertram, A., Butz, W., Dettling, F., Drotleff, J., Elsner, C., Fee, E., Gabler, C., Galander, C., Hargita, Y., Herbener, R., Hermann, T., Jäger, F., Kanthak, J., Kessler, H., Koch, Y., Kuntze, D., Lambrecht, M., Lehmann, C., Lehmann, H., Leuthold, S., Lünenbürger, B., Lütkehus, I., Martens, K., Müller, F., Müschen, K., Nissler, D., Plickert, S., Purr, K., Reichart, A., Reichel, J., Salecker, H., Schneider, S., Schuberth, J., Schulz, D., Sieck, M., Strenge, U., Westermann, B., Werner, K., Winde, C., Wunderlich, D., Zietlow, B., 2014. Treibhausgasneutrales Deutschland im Jahr 2050 (Climate Change 07/2014). Technical Report. Dessau-Roßlau.

[10] Bundesministerium für Wirtschaft und Energie, 2017. Zahlen und Fakten. Energiedaten. URL: http://www.bmwi.de/Redaktion/DE/Artikel/Energie/energiedaten-gesamtausgabe.html.

[11] Bundesnetzagentur, 2016. Genehmigung des Szenariorahmens für die Netzentwicklungspläne Strom 2017-2030. Technical Report. Bonn.

[12] Bundesverband der deutschen Gas- und Wasserwirtschaft (BGW), 2006. Praxisinformation P 2006/8 Gastransport/Betriebswirtschaft. Anwendung von Standardlastprofilen zur Belieferung nicht-leistungsgemessener Kunden. Technical Report. Berlin.

[13] Bürger, V., Hesse, T., Quack, D., Palzer, A., Köhler, B., Henkel, S., Engelmann, P., 2016. Klimaneutraler Gebäudebestand 2050 (Climate Change 06/2016). Technical Report. Dessau-Roßlau.

[14] Buttler, A., Hentschel, J., Kahlert, S., Angerer, M., 2015. Statusbericht Flexibilitätsbedarf im Stromsektor. Technical Report. München.

[15] Deutscher Wetterdienst, . WESTE-XL. URL: https://www.dwd.de/DE/leistungen/weste/westexl/weste{_}xl.html?nn=342632.

[16] Duffie, J.A., Beckman, W.A., 2013. Solar Engineering of Thermal Processes. 4th ed., John Wiley & Sons, Inc., New Jersey.

[17] Eckstein, S., Buddeke, M., Merten, F., 2015. RESTORE2050. Europäischer Lastgang 2050. Projektbericht. Technical Report. Wuppertal.

[18] Elsner, P., Fischedick, M., Sauer, D.U., Erlach, B., Lunz, B., 2015. Flexibilitätskonzepte für die Stromversorgung 2050. Technologien - Szenarien - Systemzusammenhänge (Analyse aus der Schriftenreihe Energiesysteme der Zukunft). Technical Report. München.

[19] ENTSO-E - European Network of Transmission System Operators for Electricity, 2017. Power Statistics. URL: https://www.entsoe.eu/about-entso-e/inside-entso-e/contact-entso-e/Pages/default.aspx.

[20] Gerhardt, N., Sandau, F., Scholz, A., Hahn, H., Schumacher, P., Sager, C., Bergk, F., Kämper, C., Knörr, W., Kräck, J., Lambrecht, U., Antoni, O., Hilpert, J., Merkel, K., Müller, T., 2015. Interaktion EE-Strom, Wärme und Verkehr. Technical Report. Kassel, Heidelberg, Würzburg.

[21] Görner, K., Sauer, D.U., 2016. Konventionelle Kraftwerke. Technologiesteckbrief zur Analyse "Flexibilitätskonzepte für die Stromversorgung 2050" (Schriftenreihe Energiesysteme der Zukunft). Technical Report. München.

[22] Hamburg University of Technology, 2018. TransiEnt Library. URL: https://www.tuhh.de/transient-ee/en/.

[23] Henning, H.M., Palzer, A., 2015. Was kostet die Energiewende? Wege zur Transformation des deutschen Energiesystems bis 2050. Technical Report. Freiburg.

[24] IKM, 2018. Initiativkreis Europäische Metropolregionen in Deutschland. URL: http://www.deutsche-metropolregionen.org/.

[25] Kopp, M., Coleman, D., Stiller, C., Scheffer, K., Aichinger, J., Scheppat, B., 2017. Energiepark Mainz: Technical and economic analysis of the worldwide largest Power-to-Gas plant with PEM electrolysis. International Journal of Hydrogen Energy 42, 13311–13320. doi:10.1016/j.ijhydene.2016.12.145.

[26] Loga, T., Stein, B., Diefenbach, N., Born, R., 2015. Deutsche Wohngebäudetypologie. Beispielhafte Maßnahmen zur Verbesserung der Energieeffizienz von typischen Wohngebäuden. 2nd ed. ed., Institut Wohnen und Umwelt GmbH, Darmstadt.

[27] Modelica Association, 2018. Modelica and the Modelica Association. URL: https://www.modelica.org/.

[28] Nitsch, J., Pregger, T., Naegler, T., Heide, D., de Tena, D.L., Trieb, F., Scholz, Y., Gerhardt, N., Sterner, M., Trost, T., von Oehsen, A., Schwinn, R., Pape, C., Hahn, H., Wenzel, B., 2012. Langfristszenarien und Strategien für den Ausbau der Erneuerbaren Energien in Deutschland bei Berücksichtigung der Entwicklung in Europa und global. Schlussbericht. Technical Report. Stuttgart, Kassel, Teltow.

[29] Osório, T., Carvalho, M.J., 2014. Testing of solar thermal collectors under transient conditions. Solar Energy 104, 71–81. doi:10.1016/j.solener.2014.01.048.
[30] Palzer, A., 2016. Sektorübergreifende Modellierung und Optimierung eines zukünftigen deutschen Energiesystems unter Berücksichtigung von Energieeffizienzmaßnahmen im Gebäudesektor. Fraunhofer Verlag, Stuttgart.
[31] Pape, C., Gerhardt, N., Härtel, P., Scholz, A., Schwinn, R., Drees, T., Maaz, A., Sprey, J., Breuer, C., Moser, A., Sailer, F., Reuter, S., Müller, T., 2014. Roadmap Speicher. Speicherbedarf für erneuerbare Energien - Speicheralternativen - Speicheranreiz - Überwindung rechtlicher Hemmnisse. Endbericht. Technical Report. Kassel, Aachen, Würzburg.
[32] Quaschning, V., 2015. Regenerative Energiesysteme. Technologie - Berechnung - Simulation. 9th ed., Carl Hanser Verlag GmbH & Co. KG, München.
[33] Rippel, K.M., Wiede, T., Meinecke, M., König, R., 2017. Netzentwicklungsplan Strom 2030, Version 2017. Zweiter Entwurf. Technical Report. Berlin, Dortmund, Bayreuth, Stuttgart.
[34] Schlereth, D., 2015. Kinetic and Reactor Modeling for the Methanation of Carbon Dioxide. Phd thesis. Technische Universität München.
[35] Schlesinger, M., Hofer, P., Kemmler, A., Kirchner, A., Koziel, S., Ley, A., Piégsa, A., Seefeldt, F., Straßburg, S., Weinert, K., Lindenberger, D., Knaut, A., Malischek, R., Nick, S., Panke, T., Paulus, S., Tode, C., Wagner, J., Lutz, C., Lehr, U., Ulrich, P., 2014. Entwicklung der Energiemärkte – Energiereferenzprognose. Endbericht. Technical Report. Basel, Köln, Osnabrück.
[36] Stolzenburg, K., Hamelmann, R., Wietschel, M., Genoese, F., Michaelis, J., Lehmann, J., Miege, A., Krause, S., Sponholz, C., Donadei, S., Crotogino, F., Acht, A., Horvath, P.L., 2014. Integration von Wind-Wasserstoff-Systemen in das Energiesystem. Abschlussbericht. Technical Report. Berlin.
[37] TenneT TSO GmbH, 2017. Tatsächliche und prognostizierte Windenergieeinspeisung. URL: https://www.tennettso.de/site/Transparenz/veroeffentlichungen/netzkennzahlen/tatsaechliche-und-prognostizierte-windenergieeinspeisung.
[38] Teske, S., Sawyer, S., Schäfer, O., Pregger, T., Simon, S., Naegler, T., Schmid, S., Özdemir, D., Pagenkopf, J., Kleiner, F., Rutovitz, J., Dominish, E., Downes, J., Ackermann, T., Brown, T., Boxer, S., Baitelo, R., Rodrigues, L.A., 2015. energy [R]evolution. A Sustainable World Energy Outlook 2015. Technical Report. Amsterdam, Brussels.
[39] University of California, 2018. Open source library for building energy and control systems. URL: http://simulationresearch.lbl.gov/modelica/.
[40] Vattenfall GmbH, 2018. Wasserkraft in Deutschland. URL: https://corporate.vattenfall.de/uber-uns/geschaftsfelder/erzeugung/wasserkraft/wasserkraft-in-deutschland-psw/.
[41] Verein Deutscher Ingenieure, 2012. VDI 2067 Part 1. Economic efficiency of building installations. Fundamentals and economic calculation. Beuth Verlag GmbH, Berlin.
[42] Viessmann Werke GmbH & Co. KG, 2017. Vitosol 100-FM Datenblatt.
[43] Wietschel, M., Arens, M., Dötsch, C., Herkel, S., Krewitt, W., Markewitz, P., Möst, D., Scheufen, M., 2010. Energietechnologien 2050 - Schwerpunkte für Forschung und Entwicklung: Technologienbericht.
[44] Ziems, C., Meinke, S., Nocke, J., Weber, H., Hassel, E., 2012. Kraftwerksbetrieb bei Einspeisung von Windparks und Photovoltaikanlagen - Abschlussbericht zum Forschungsvorhaben. Technical Report. Rostock.